Estimate of the dark matter distribution in galaxy cluster MACS J1206 through a free-form strong lensing analysis

Alberto Manjón García

in collaboration with

Jose M. Diego, Diego Herranz & Daniel Lam

Instituto de Fisica de Cantabria
Universidad de Cantabria: *manjon@ifca.unican.es*

UNIVERSIDAD DE CANTABRIA

Instituto de Física de Cantabria

CSIC CONSEJO SUPERIOR DE INVESTIGACIONES CIENTÍFICAS

EXCELENCIA MARÍA DE MAEZTU

Introduction

What?

- We have performed a free-form analysis on strong lensing data from galaxy cluster MACS J1206.2-0847 (J1206) in order to estimate its inner total mass distribution and the position of the background sources.
- The stellar mass of the brightest cluster galaxy (BCG) was estimated and subtracted from the total mass distribution so as to achieve a measure of the dark matter density profile in the inner core of J1206.

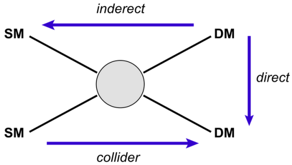

Why?

- Inner region of galaxy clusters contains the largest densities of dark matter.
- If dark matter has a small cross section for interaction, deviations from pure collisionless dark matter particle models are expected to appear here.
- Inner dark matter density profile in galaxy clusters provides a test of dark matter models.

Strong lensing approach

The central mass profile of galaxy clusters can be inferred in several ways:

Stellar kinematics
SZ or X-ray emission
Strong lensing
Weak lensing

} Cover the full range from 10 kpc to 1 Mpc scale

Strong lensing

- Multiple images of background sources.
- Images are magnificated and strongly distorted into rings/arcs.
- Some distinguishable features (knots) might be observed within some multiple images.
- Images appear typically near the Einstein radius of the lens (tens of kpc)
- But can also appear close to the radial critical curve (few kpc from center)

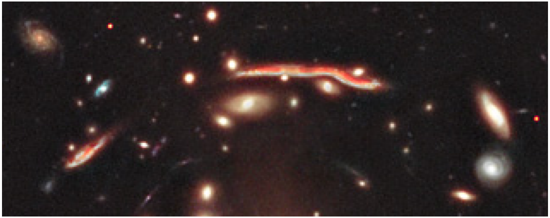

Previous analysis of MACS J1206

Strong lensing data usually contain a few arcs $\longrightarrow$ Insufficient to constrain the mass distribution without a parametrization

Parametric models have become the standard tool for modelling strong-lensing in clusters.

These models rely on assumptions or priors about the cluster mass distribution.

This cluster has been analyzed several times since its discovery on June 15th 1999:

1. Ebeling et al. (2009): X-ray and strong-lensing analysis. Parametric model.
   2 counter-images belonging to 1 background source (7 SL constraints).
2. Zitrin et al. (2012): Strong-lensing analysis. Parametric model.
   32 secure multiple images belonging to 9 sources. (32 SL constraints).
3. Umetsu et al. (2012): Weak and strong-lensing analysis.
   Main model is parametric. [Re-analysis of Zitrin et al. (2012)]
   Secondary analyses are both parametric and non-parametric.
4. Eichner et al. (2013): Strong-lensing analysis. Parametric model.
   50 multiple images belonging to 13 sources. (50 SL constraints)
5. Caminha et al. (2017): Strong-lensing analysis. Parametric model.
   82 spectroscopic multiple images belonging to 27 sources. (82 SL constraints)

Galaxy cluster MACS J1206

MACS J1206 is a massive X-ray luminous cluster at $z = 0.439$

X-ray/optical images
Galaxies kinematics
} **Dynamically relaxed with a pronounced X-ray peak at the BCG**

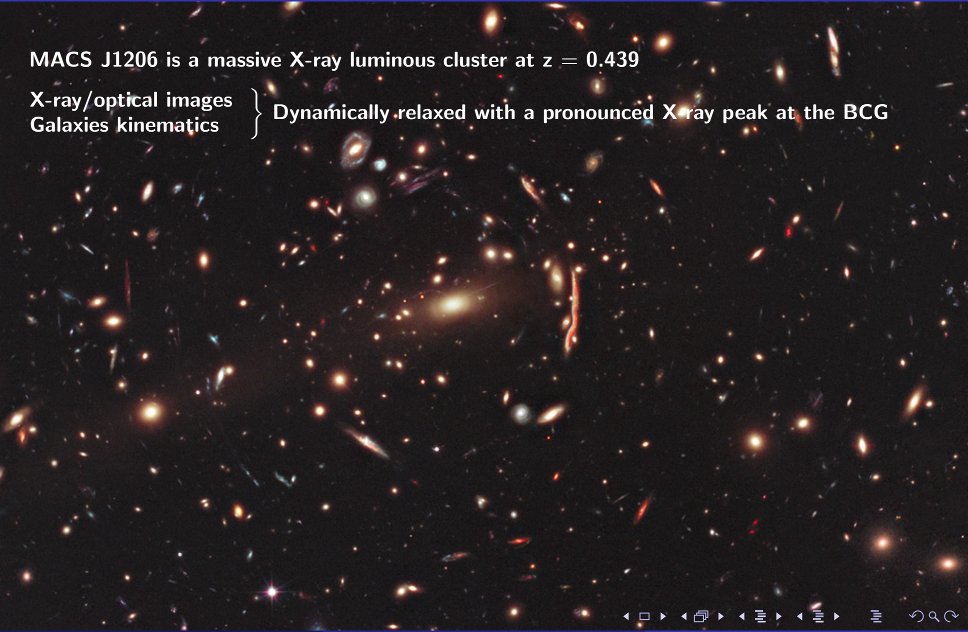

Why did we choose MACS J1206?

- Almost only parametric analyses have been used to derive its mass distribution.
- 82 secure images of 27 sources at z = 1.01-6.01 identified with CLASH-VLT and MUSE.
- 11 multiple images are found within 50 kpc of the BCG.
- Two arcs (one straight and other curved) can clearly be seen arising from the BCG.
- This cluster has a giant arc which is bent around several cluster members.

Data: Images and cluster galaxies

- Public imaging data from ACS and WFC3 Hubble instruments.
- Optical: F275W, F336W, F390W, F475W, F606W, F775W, F814W and F850LP.
- IR: F105W, F110W, F125W, F140W and F160W.
- 54 galaxies spectroscopically confirmed with CLASH-VLT/VIMOS ($0.425 \leq z \leq 0.453$)

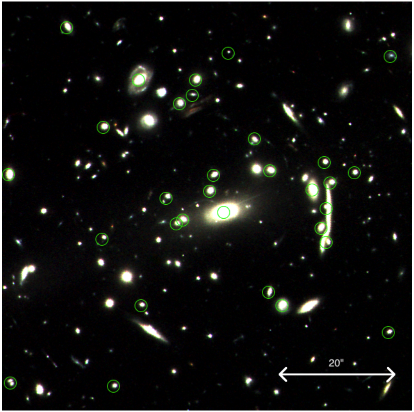

Data: Multiple-lensed images

- We started following the multiple-image identifications from Caminha et al. (2017).
- 97 spectroscopic multiple images belonging to 27 sources at $z = [1.01, 6.06]$.
- z_{spec} from CLASH-VLT and MUSE.

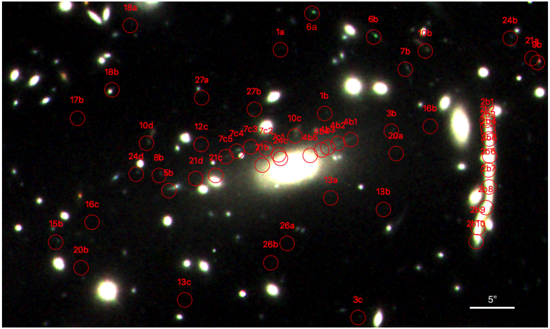

Multiple lensed images close to the BCG.

ID	z_{spec}
1	1.0121
2	1.0369
3	1.0433
4	1.4248
5	1.4254
6	1.4255
7	1.4257
8	1.4864
9	1.9600
10	2.5393
11	3.0358
12	3.3890
13	3.3961
14	3.7531

ID	z_{spec}
15	3.7611
16	3.7617
17	3.8224
18	4.0400
19	4.0520
20	4.0553
21	4.0718
22	4.2913
23	4.7293
24	5.6984
25	5.7927
26	6.0106
27	6.0601

Weak and Strong Lensing Analysis Package (WSLAP)

Free-form method to reconstruct the cluster mass distribution:

- No initial assumption or prior information about the underlying mass distribution.
- Condition: Requires a sufficiently large number of constraints (lensed images) to work.

- Data: Observed positions $\vartheta = (\vartheta_x, \vartheta_y)$ of the background sources.
- Aim: Estimate $\Sigma(\vartheta)$ of lens and true positions $\beta = (\beta_x, \beta_y)$ of the background galaxies.
- Number of strongly lensed arcs with known z has to be large enough.

$$\begin{pmatrix} \vartheta_x \\ \vartheta_y \end{pmatrix} = \begin{pmatrix} \Upsilon_x & 1 & 0 \\ \Upsilon_y & 0 & 1 \end{pmatrix} \begin{pmatrix} \Sigma \\ \beta_x \\ \beta_y \end{pmatrix} \rightarrow \quad \Theta = \Gamma X \rightarrow \quad \text{Inversion Method (QADP)}$$

The solution of this equation is found after minimizing a quadratic function of X.

Θ: $2N_\vartheta$ vector with (x,y) positions of the observed arcs $\longrightarrow$ observables.
Γ: $2N_\vartheta \times (N_c + N_g + 2N_s)$ matrix with all known physics and geometry.
X: $(N_c + N_g + 2N_s)$ vector with β positions and m_i $\longrightarrow$ unknowns

Weak and Strong Lensing Analysis Package (WSLAP)

$$\Sigma(\vartheta) = \left\{ \begin{array}{l} \text{- A soft component composed of a superposition of } N_c \text{ basis functions on a grid.} \\ \text{- A compact component that accounts for the mass associated with the galaxies.} \end{array} \right\}$$

Soft component

- Gaussian functions are used.
- Good compromise between the desired compactness and smoothness.
- Fast analytical computation of the integrated mass for a given radius.

Compact component

- Split into independent layers $\rightarrow$ Constrain separately the mass of different galaxies.
- Modelled by assigning to each galaxy a mass proportional to its light distribution.
- This mass is later re-adjusted in the optimization process.

We explored different models by changing the assumptions for these two components:

Number of layers, **Light-to-mass ratio** & **Grid definition**

Configurations considered for the compact component

* N_g is the number of layers and l/m is the light-to-mass ratio assumed.

Compact component configuration:

- Case 1: $N_g = 2 \longrightarrow$ BCG ($l/m = 1$) & 53 galaxies ($l/m = 1$)
- Case 2: $N_g = 1 \longrightarrow$ BCG ($l/m = 1$) + 53 galaxies ($l/m = 1$)
- Case 3: $N_g = 1 \longrightarrow$ BCG ($l/m = \frac{1}{2}$) + 53 galaxies ($l/m = 1$)
- Case 4: $N_g = 1 \longrightarrow$ BCG ($l/m = \frac{1}{3}$) + 53 galaxies ($l/m = 1$)
- Case 5: $N_g = 1 \longrightarrow$ 53 galaxies ($l/m = 1$)

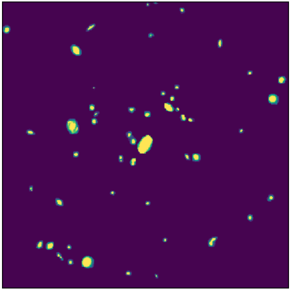

Case 2

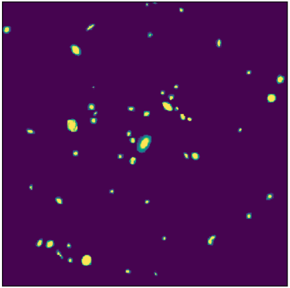

Case 4

Configurations considered for the soft component

Soft component configuration:

- Regular grid with $N_c = 1024$ cells.
- Adaptive grid with $N_c = 406$ cells.
- Adaptive grid with $N_c = 480$ cells.

Grid / Case	1	2	3	4	5
406	1a	2a	3a	4a	5a
480	1b	2b	3b	4b	5b
1024	1c	2c	3c	4c	-

14 different models considered.

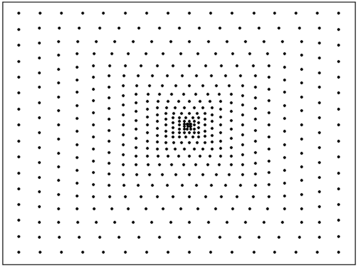

Adaptive grid with $N_c = 480$.

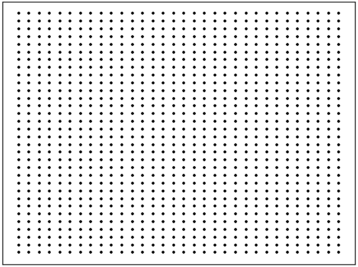

Regular grid with $N_c = 1024$.

Reconstruction of counter-image 2b

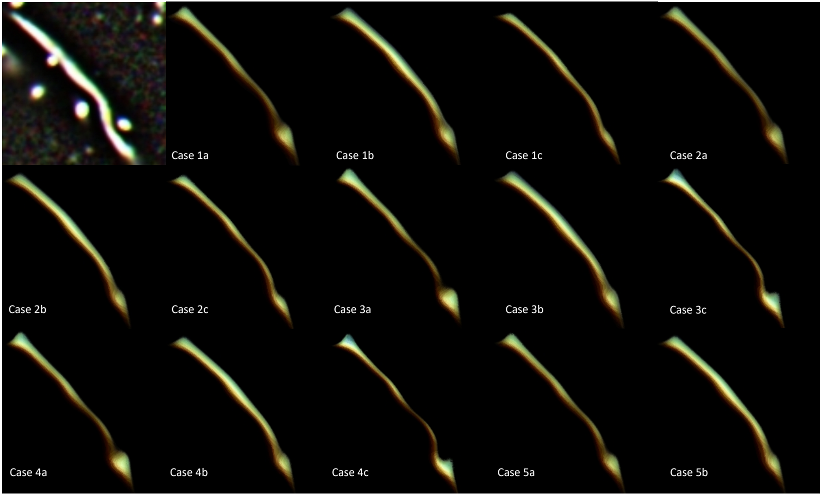

Reconstruction of counter-image 4b

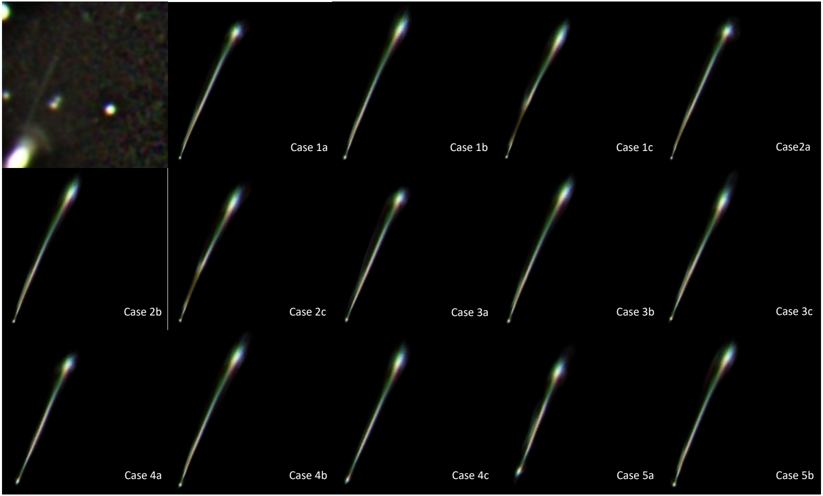

Reconstruction of counter-image 7c

What model is able to better reproduce arcs 4b and 7c?

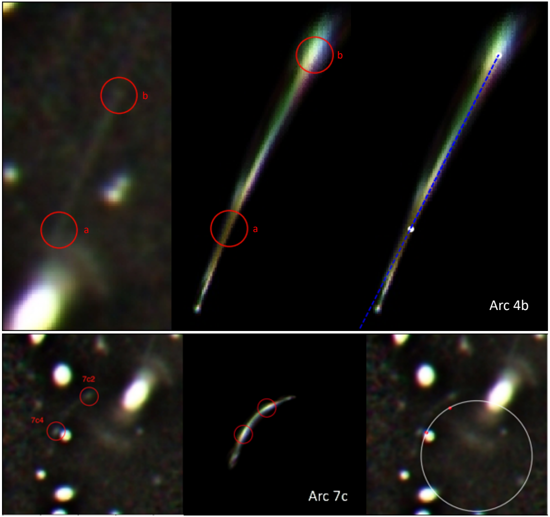

- Counter-image 4b is fit to a straight line. Counter-image 7c is fit to a circle.
- We perform a χ^2 fit statistic on 5 parameters for each model considered.

Results

- We find that Case 2c ($N_g = 1$, $l/m = 1$ and $N_c = 1024$ cells) is the model that performs a more accurate reconstruction of counter-images 4b and 7c.
- The profile is not flat in the center which comes to confirm the relaxed state of the cluster.
- The dark matter density profile for this model is well fitted by a NFW profile.
- This good fit would support collisionless dark matter models.

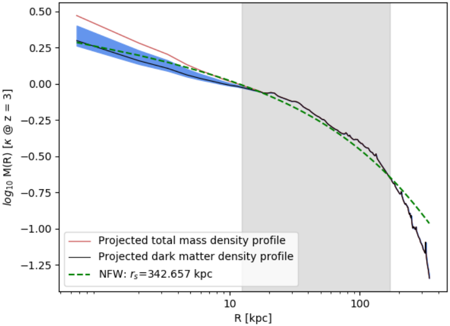

Total mass and dark matter density profiles

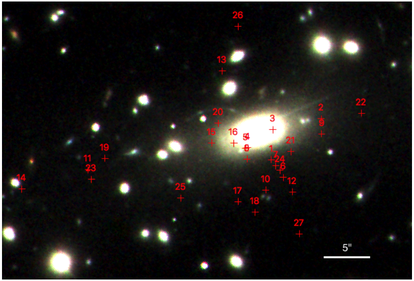

Estimated positions of the background sources

Conclusions

- We conclude that Case 2c ($N_g = 1$, $l/m = 1$ and $N_c = 1024$ cells) is the model that performs a more accurate reconstruction of counter-images 4b and 7c.
- The profile is not flat in the center coming to confirm the relaxed state of the cluster.
- The dark matter density profile for this model is well reproduced by a NFW profile.
- This good fit would support collisionless dark matter models.
- The best model predicts all lensed images from Caminha et al. 2017 not used because of being close to massive galaxies or having no identification in the MUSE and HST data.
- The model also predicts new counter-images for some systems (14, 18 and 21).

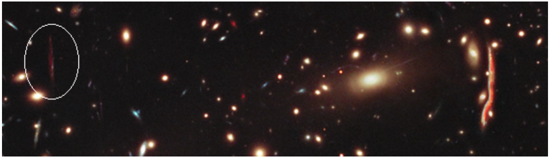

Elongated structure predicted as a counter-image of system 14.

Thanks for your attention!

BACK UP

Estimation of the stellar component of the BCG

- Photometry of the BCG measured by running SExtractor over several filters of the cluster
- F160W is used for source detection, segmentation and definition of isophotal apertures
- Fit synthetic stellar population spectra to the observed SED with FAST (Kriek et al. 2009)
- The stellar mass of the best-fit spectrum is $3.61^{+0.57}_{-1.98} \times 10^{11}$ (3σ interval)